Advanced Composite Materials
Publication details, including instructions for authors and subscription information:
http://www.tandfonline.com/loi/tacm20

Delamination originating from transverse crack tips in laminates under mechanical loadings

Kyohei Kondo [a], Keishiro Yoshida [b] & Kazuhiro Yagi [c]

[a] Department of Aeronautics and Astronautics, University of Tokyo, 7-3-1 Hongo, Bunkyo-ku, Tokyo 113-8656, Japan

[b] Engineering Department, Japan Air Lines Co., Ltd., Maintenance Center, Tokyo International Airport, Haneda, Ota-ku, Tokyo 144, Japan

[c] Space Systems Department, Aerospace Division, Nissan Motor Co., Ltd., 900 Fujiki, Tomioka-shi, Gunma 370-2398, Japan

Version of record first published: 02 Apr 2012.

Adv. Composite Mater., Vol. 8, No. 2, pp. 153–165 (1999)

Delamination originating from transverse crack tips in laminates under mechanical loadings

KYOHEI KONDO [1,*], KEISHIRO YOSHIDA [2] and KAZUHIRO YAGI [3]

[1] *Department of Aeronautics and Astronautics, University of Tokyo, 7-3-1 Hongo, Bunkyo-ku, Tokyo 113-8656, Japan*
[2] *Engineering Department, Japan Air Lines Co., Ltd., Maintenance Center, Tokyo International Airport, Haneda, Ota-ku, Tokyo 144, Japan*
[3] *Space Systems Department, Aerospace Division, Nissan Motor Co., Ltd., 900 Fujiki, Tomioka-shi, Gunma 370-2398, Japan*

Received 7 July 1998; accepted 7 August 1998

Abstract—A singular finite element method is formulated utilizing the asymptotic solutions for displacements and stresses near the tip of the interface crack between dissimilar anisotropic materials and the variational principle of a hybrid functional. The interfacial crack problem can be analyzed by the singular hybrid element at the interfacial crack tip and the conventional displacement-based elements surrounding the crack element.

Analyzing a small central interfacial crack between two large anisotropic composite layers with different fiber orientations subjected to uniform tensile load, we demonstrate that the present numerical solutions are in good agreement with the analytical ones for an interfacial crack between two semi-infinite anisotropic solids. Then, we apply the present method for the analysis of delamination originating from the transverse crack tip in laminates under plane strain extension, antiplane shear and plane strain bending.

Keywords: Interface crack; delamination; stress singularity; hybrid singular element; energy release rate.

1. INTRODUCTION

Delamination is the most commonly observed failure mode in composite laminates under mechanical and hygrothermal loadings. Onset and growth of the delamination can be characterized by the fracture mechanics based on the singular stress distribution near the crack tip. The stress and displacement fields at the vicinity of interfacial crack can be analyzed by the conventional displacement finite element method [1, 2] or the singular hybrid finite element method [3, 4]. Kim and Im [4]

*To whom correspondence should be addressed.

formulated a hybrid singular element for the analysis of interfacial crack in cross-ply laminates based on the asymptotic solution for the stress and displacement fields utilizing the Stroh formalism extended by Ting [5].

In the present paper, we develop a singular hybrid element for studying the interfacial crack between two composite layers with arbitrary fiber orientations. The fundamental solutions for the displacements and stresses at the tip of interfacial crack between dissimilar anisotropic materials representing unidirectional fiber-reinforced composites with arbitrary fiber orientations are reviewed based on the Stroh formalism [5]. Then, the singular crack element is formulated utilizing the elasticity solutions and a hybrid variational principle. The delamination problem can be analyzed by the singular element at the crack tip and the surrounding displacement finite elements.

We apply the present method for the analysis of a small central crack between two large unidirectional composite layers simulating a central crack between dissimilar semi-infinite anisotropic materials under uniform tensile load, and demonstrate that the present solutions are in good agreement with the analytical ones. Then, we analyze delamination origination from the tip of transverse crack in laminate plates under plane strain extension, antiplane shear and plane strain bending. Comparisons of the present numerical solutions with the results by the displacement finite element method show the accuracy and efficiency of the present hybrid finite element method. As a fracture mechanic parameter, the potential energy release rate is calculated as a function of delamination length directly from the singular hybrid element calculation.

2. ASYMPTOTIC SOLUTIONS FOR DISPACEMENTS AND STRESSES NEAR INTERFACIAL CRACK TIP

In the generalized plane strain state, displacements are given by

$$u_i = U_i(x_\sigma). \tag{1}$$

We use the convention that all Latin indices take the values 1, 2, 3, and all Greek indices the values 1, 2. The general solutions for stress and displacement fields in unidirectional composite layers with arbitrary fiber orientations are presented. The near-field conditions are imposed to get the eigenvalue equations, which yield the asymptotic solutions for stresses and displacements, including the stress singularities at the crack tip.

2.1. Two-dimensional anisotropic elasticity

If we assume that the general solution for displacements is expressed as

$$u_k = a_k f(z), \qquad z = x_1 + p x_2, \tag{2}$$

the six eigenvalues and the corresponding six eigenvectors are given by

$$p_\alpha,\ p_{\alpha+3} = \overline{p}_\alpha, \qquad \mathbf{a}_\alpha, \mathbf{a}_{\alpha+3} = \overline{\mathbf{a}}_\alpha, \qquad (\mathrm{Im}[p_\alpha] > 0, \quad \alpha = 1, 2, 3), \tag{3}$$

where Im stands for the imaginary part and the overbar denotes the complex conjugate. The displacements are expressed as

$$\mathbf{u} = \sum_{\alpha=1}^{3} \left\{ \mathbf{a}_\alpha f_\alpha(z_\alpha) + \overline{\mathbf{a}}_\alpha f_{\alpha+3}(\overline{z}_\alpha) \right\}, \quad z_\alpha = x_1 + p_\alpha x_2, \tag{4}$$

and the stresses take the form

$$\begin{aligned} \sigma_{i1} &= -\sum_{\alpha=1}^{3} \left\{ p_\alpha b_{i\alpha} \frac{\mathrm{d}}{\mathrm{d}z_\alpha} f_\alpha(z_\alpha) + \overline{p}_\alpha \overline{b}_{i\alpha} \frac{\mathrm{d}}{\mathrm{d}\overline{z}_\alpha} f_{\alpha+3}(\overline{z}_\alpha) \right\} \\ \sigma_{i2} &= \sum_{\alpha=1}^{3} \left\{ b_{i\alpha} \frac{\mathrm{d}}{\mathrm{d}z_\alpha} f_\alpha(z_\alpha) + \overline{b}_{i\alpha} \frac{\mathrm{d}}{\mathrm{d}\overline{z}_\alpha} f_{\alpha+3}(\overline{z}_\alpha) \right\}, \end{aligned} \tag{5}$$

where

$$b_{i\alpha} = (C_{k1i2} + p_\alpha C_{i2k2}) a_{k\alpha} = -\frac{1}{p_\alpha}(C_{i1k1} + p_\alpha C_{i1k2}) a_{ik}. \tag{6}$$

2.2. Displacements and stresses near interfacial crack tip

If we assume a power-type function for $f(z)$ in equation (2) as

$$f(z) = \frac{c z^{\delta+1}}{\delta + 1}, \quad \mathrm{Re}[\delta] > -1, \tag{7}$$

near the crack tip as shown in Fig. 1, we have

$$f_\alpha(z_\alpha) = q_\alpha \frac{z_\alpha^{\delta+1}}{\delta+1}, \qquad f_{\alpha+3}(\overline{z}_\alpha) = h_\alpha \frac{\overline{z}_\alpha^{\delta+1}}{\delta+1}, \quad (\alpha = 1, 2, 3). \tag{8}$$

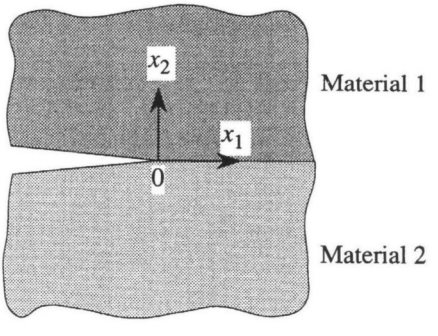

Figure 1. Semi-infinite crack between dissimilar anisotropic materials.

From the stress conditions on the crack surface and the continuity conditions on the interface, we get

$$\delta_n^I = -\frac{1}{2} + n + i\gamma, \quad \bar{\delta}_n^I = -\frac{1}{2} + n - i\gamma, \quad \delta_n^R = -\frac{1}{2} + n,$$
$$\delta_n^{N_1} = \delta_n^{N_2} = \delta_n^{N_3} = n, \quad (n = 0, 1, 2, \ldots). \tag{9}$$

It follows from equations (4), (5), and (8) that the displacements and stresses are given by

$$u_i^{(k)} = \sum_{n=0}^{\infty} \left[\beta_n^{I_1} \operatorname{Re}\left[\varphi_{in}^{I(k)}\right] + \beta_n^{I_2} \operatorname{Im}\left[\varphi_{in}^{I(k)}\right] + \beta_n^R \operatorname{Re}\left[\varphi_{in}^{R(k)}\right] + \sum_{j=1}^{3} \beta_n^{N_j} \operatorname{Re}\left[\varphi_{in}^{N_j(k)}\right] \right], \quad (k = 1, 2), \tag{10}$$

$$\sigma_{i1}^{(k)} = \sum_{n=0}^{\infty} \left[\beta_n^{I_1} \operatorname{Re}\left[X_{in}^{I(k)}\right] + \beta_n^{I_2} \operatorname{Im}\left[X_{in}^{I(k)}\right] + \beta_n^R \operatorname{Re}\left[X_{in}^{R(k)}\right] + \sum_{j=1}^{3} \beta_n^{N_j} \operatorname{Re}\left[X_{in}^{N_j(k)}\right] \right],$$
$$\sigma_{i2}^{(k)} = \sum_{n=0}^{\infty} \left[\beta_n^{I_1} \operatorname{Re}\left[\psi_{in}^{I(k)}\right] + \beta_n^{I_2} \operatorname{Im}\left[\psi_{in}^{I(k)}\right] + \beta_n^R \operatorname{Re}\left[\psi_{in}^{R(k)}\right] + \sum_{j=1}^{3} \beta_n^{N_j} \operatorname{Re}\left[\psi_{in}^{N_j(k)}\right] \right], \quad (k = 1, 2). \tag{11}$$

3. HYBRID FINITE ELEMENT FORMULATION

A modified hybrid Hellinger-Reissner variational functional is derived. Then, based on the hybrid functional and the asymptotic solutions for the displacements and stresses near the crack tip, the stiffness matrix for the crack element is formulated, and the numerical procedure to obtain the potential energy release rate at the crack tip is presented.

3.1. Modified hybrid Hellinger-Reissner principle

The functional of the hybrid Hellinger-Reissner principle is given by

$$\Pi_{Rh} = \sum_m \left[\iint_{A_m} \left\{ \frac{1}{2}\sigma_{ij}(u_{i,j} + u_{j,i}) - U_c(\sigma_{ij}) \right\} \mathrm{d}A - \int_{s_m} T_i(u_i - \tilde{u}_i)\,\mathrm{d}s - \int_{(s_u)_m} T_i(u_i - \bar{u}_i)\,\mathrm{d}s - \int_{(s_\sigma)_m} \bar{T}_i u_i\,\mathrm{d}s \right], \tag{12}$$

where A_m is the area of element, s_m is the interelement boundary, $(s_u)_m$ the boundary where displacements are prescribed, $(s_\sigma)_m$ the boundary where tractions are prescribed, and $\tilde{u}_i$ are displacements defined along the interelement boundary. If we assume that there is not the boundary $(s_u)_m$ and

$$\overline{T}_i = 0 \quad \text{on } (s_\sigma)_m, \tag{13}$$

and that the stresses satisfy the equilibrium equations and the compatibility conditions, the functional of the modified Hellinger-Reissner principle takes the form

$$\begin{aligned}\Pi_{mRh} &= \sum_m \left[\int_{s_m} T_i \tilde{u}_i \, \mathrm{d}s - \frac{1}{2} \int_{s_m} T_i u_i \, \mathrm{d}s \right] \\ &= \sum_m \left[\int_{s_m} \mathbf{T}^T \tilde{\mathbf{u}} \, \mathrm{d}s - \frac{1}{2} \int_{s_m} \mathbf{T}^T \mathbf{u} \, \mathrm{d}s \right].\end{aligned} \tag{14}$$

3.2. Stiffness matrix formulation for singular crack element

If we truncate the series expansions in equations (10) and (11) at $n = N$, we have the displacements and tractions at the interelement boundary of s_m as

$$\mathbf{u} = \mathbf{U}\boldsymbol{\beta}, \qquad \mathbf{T} = \mathbf{R}\boldsymbol{\beta}, \tag{15}$$

where

$$\begin{aligned}\boldsymbol{\beta} = \Big[&\beta_0^{I_1}, \beta_0^{I_2}, \beta_0^R, \beta_0^{N_1}, \beta_0^{N_2}, \beta_0^{N_3}, \ldots \\ &\ldots, \beta_N^{I_1}, \beta_N^{I_2}, \beta_N^R, \beta_N^{N_1}, \beta_N^{N_2}, \beta_N^{N_3} \Big].\end{aligned} \tag{16}$$

The interelement boundary displacements are expressed in terms of the nodal displacements $\mathbf{q}$ as

$$\tilde{\mathbf{u}} = \mathbf{L}\mathbf{q}. \tag{17}$$

Substituting equations (15) and (17) into equation (14), we get

$$\begin{aligned}\Pi_{mRh}^{(m)} &= \boldsymbol{\beta}^T \left[\int_{s_m} \mathbf{R}^T \mathbf{L} \, \mathrm{d}s \right] \mathbf{q} - \frac{1}{2} \boldsymbol{\beta}^T \left[\frac{1}{2} \left\{ \int_{\partial A_m} (\mathbf{R}^T \mathbf{U} + \mathbf{U}^T \mathbf{R}) \, \mathrm{d}s \right\} \right] \boldsymbol{\beta} \\ &= \boldsymbol{\beta}^T \mathbf{G}\mathbf{q} - \frac{1}{2} \boldsymbol{\beta}^T \mathbf{H} \boldsymbol{\beta}.\end{aligned} \tag{18}$$

Taking variation of $\Pi_{mRh}^{(m)}$, we obtain

$$\delta \Pi_{mRh}^{(m)} = \delta \boldsymbol{\beta}^T (\mathbf{G}\mathbf{q} - \mathbf{H}\boldsymbol{\beta}) = 0, \tag{19}$$

which gives

$$\boldsymbol{\beta} = \mathbf{H}^{-1} \mathbf{G}\mathbf{q}. \tag{20}$$

Substituting equation (20) into equation (18), the variational functional is expressed as

$$\Pi_{mRh}^{(m)} = \frac{1}{2}\mathbf{q}^T\left[\mathbf{G}^T\mathbf{H}^{-1}\mathbf{G}\right]\mathbf{q} = \frac{1}{2}\mathbf{q}^T\mathbf{k}_s\mathbf{q}, \tag{21}$$

where $\mathbf{k}_s$ is the stiffness matrix for the hybrid singular crack element.

In the present finite approach, a 17-node, hybrid crack element shown in Fig. 2 with 51 degrees of freedom is constructed. The total number N of terms in equation (15) is taken as 14. The standard quadratic interporation functions are used for the $\mathbf{L}$ in equation (17) to ensure matching of the boundary displacements of the singular hybrid element with those of the adjacent 8-node, 24 degrees of freedom, isoparametric regular elements as shown in Fig. 3.

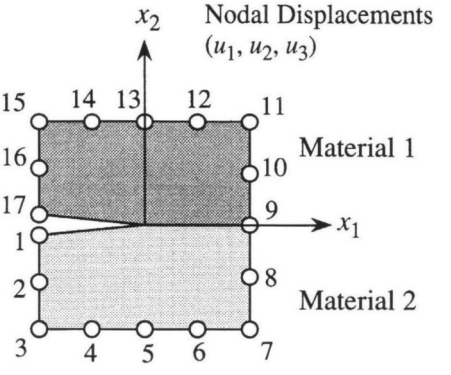

Figure 2. Hybrid singular crack element.

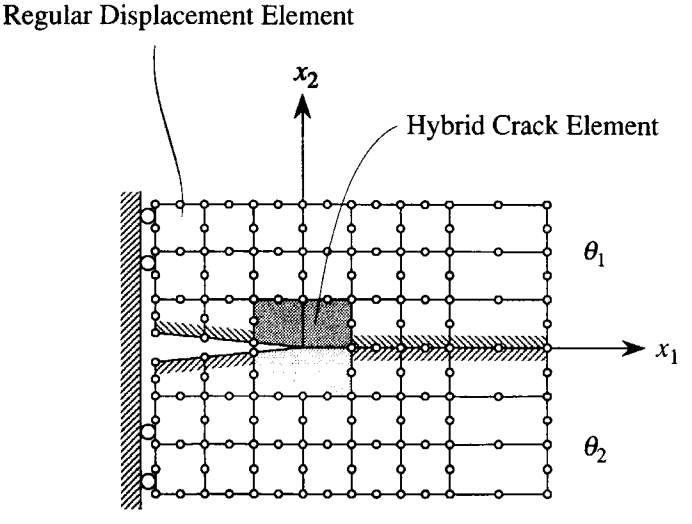

Figure 3. Discretization by hybrid crack element and regular displacement elements.

3.3. Potential energy release rate

Potential energy release rate associated with the growth of delamination of length a is given by

$$G = \lim_{\Delta a \to 0} \frac{1}{2\Delta a} \int_0^{\Delta a} \big[\sigma_{21}(r,0)\{u_1(\Delta a - r, \pi) - u_1(\Delta a - r, -\pi)\} + \sigma_{22}(r,0)\{u_2(\Delta a - r, \pi) - u_2(\Delta a - r, -\pi)\} + \sigma_{23}(r,0)\{u_3(\Delta a - r, \pi) - u_3(\Delta a - r, -\pi)\}\big]\,dr, \quad (22)$$

which is determined by the $\beta_0^{I_1}$, $\beta_0^{I_2}$, and β_0^R in equation (16) in the hybrid finite element calculation.

4. NUMERICAL RESULTS

We consider graphite epoxy laminates which are composed of laminae with the material properties:

$$E_1 = 137.90 \text{ GPa}, \quad E_2 = 14.48 \text{ GPa},$$
$$G_{12} = G_{22} = 5.86 \text{ GPa}, \quad \nu_{12} = 0.21,$$

where 1 and 2 correspond to the longitudinal and transverse directions, respectively.

As the basis of the elastic solutions for the displacement and stress fields, the stress singularity at the crack tip is studied first. And, in order to confirm the accuracy of the present finite element method, a small central crack between two large unidirectional composite layers is analyzed. Then, laminates with delamination originating from the transverse crack tip under plane strain extension, antiplane shear, and plane strain bending are investigated.

4.1. Stress singularity

For an infinite graphite epoxy composite material with the orientation angle θ, the eigenvalues p_α in equation (3) are imaginary as expressed in the form

$$p_\alpha = i\pi_\alpha.$$

The imaginary parts of the eigenvalues π_α are shown in Fig. 4 as a function of the orientation angle θ.

The order of stress singularity is given by

$$\delta = -\frac{1}{2} \pm i\gamma, -\frac{1}{2},$$

as presented in equation (9). For the interface $\theta/90$ where the delamination from transverse crack in 90° layer developes, δ's are shown in Fig. 5 as a function of θ.

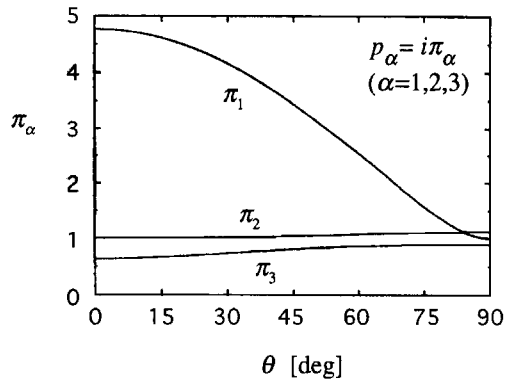

Figure 4. Eigenvalues p_α for graphite epoxy composite with orientation angle θ.

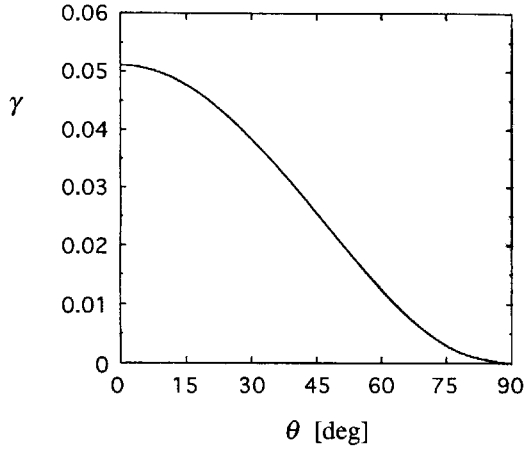

Figure 5. Imaginary parts γ of order of stress singular at interface $\theta/90°$ in laminates.

4.2. Small central crack between two large unidirectional composite layers under tensile load

To evaluate the present singular hybrid finite element solutions, we analyze a large graphite epoxy [0°/90°] laminate with a small central crack of length $2a$ subjected to uniform far field stress as shown in Fig. 6. The singular stress distributions near the crack tip are shown in Fig. 7 together with those obtained by the analytical solutions for an infinite plate [6]. It is confirmed that the present numerical solutions are in good agreement with the analytical ones.

4.3. Laminates under plane strain extention

We analyze graphite epoxy $[0°/90°]_s$ laminates under plane strain extension as shown in Fig. 8 by discretizing a quarter of the laminate with the singular element at the delamination tip and the surrounding displacement-based regular elements. The stress distributions along the interface near the delamination tip are shown in

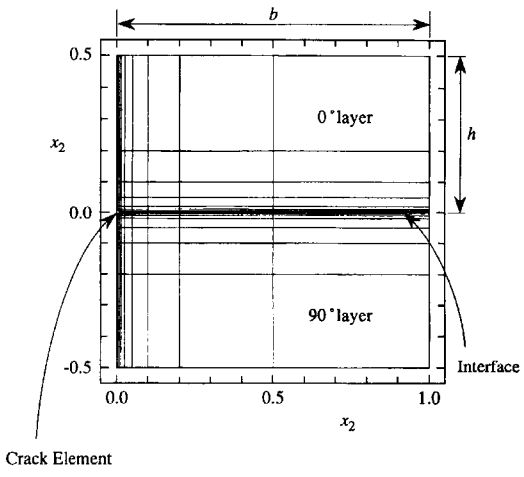

Figure 6. Graphite epoxy [0°/90°] laminate with small central crack of length $2a$ under uniform far stress σ_{22}^{∞}.

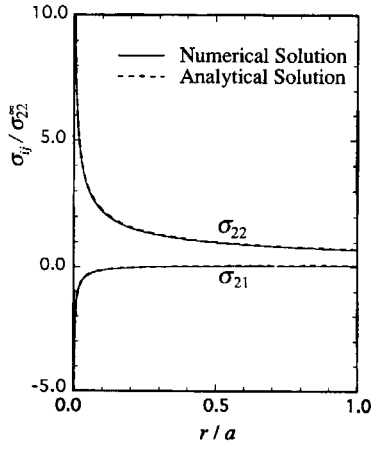

Figure 7. Singular stress distributions along interface near crack tip of graphite epoxy [0°/90°] laminate under uniform far stress σ_{22}^{∞} ($x_2 = 0, r = x_1 - a$).

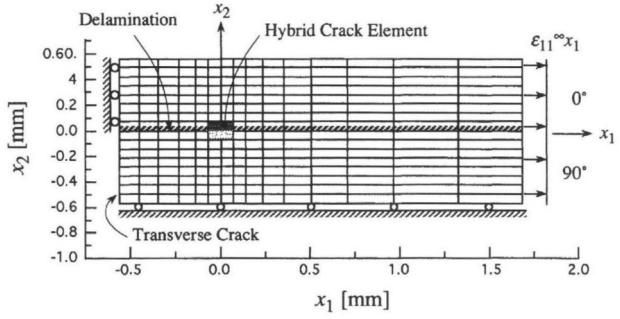

Figure 8. Graphite epoxy $[0°/90°]_S$ laminate with delamination originating from transverse crack tip under plane strain extension.

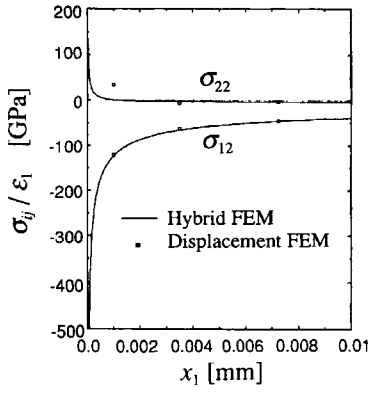

Figure 9. Stress distributions along interface of graphite epoxy $[0°/90°]_S$ laminate with delamination originating from transverse crack tip under plane strain extension.

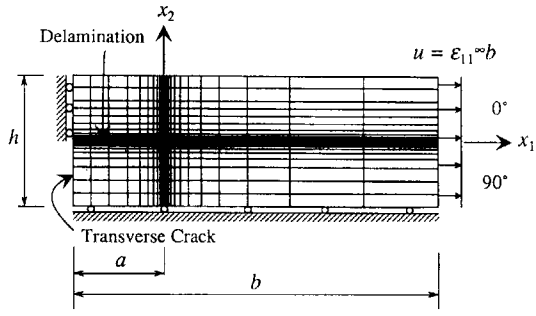

Figure 10. Discretization for displacement finite element analysis of graphite epoxy $[0°/90°]_S$ laminate with delamination originating from transverse crack tip under plane strain extension.

Fig. 9 together with those obtained by the displacement finite element method with fine descretization, as illustrated in Fig. 10. The potential energy release rates are shown in Fig. 11 as a function of the delamination length for various aspect ratios of the laminates. In Fig. 11 are also shown the asymptotic values of the energy release rates obtained from the superposition method based on the classical lamination plate theory [7].

4.4. Laminate under antiplane shear

We analyze graphite epoxy $[0°/90°]_S$ laminates under antiplane shear as shown in Fig. 12. The stress distributions along the interface near the delamination tip are shown in Fig. 13, together with those obtained by the displacement finite element method.

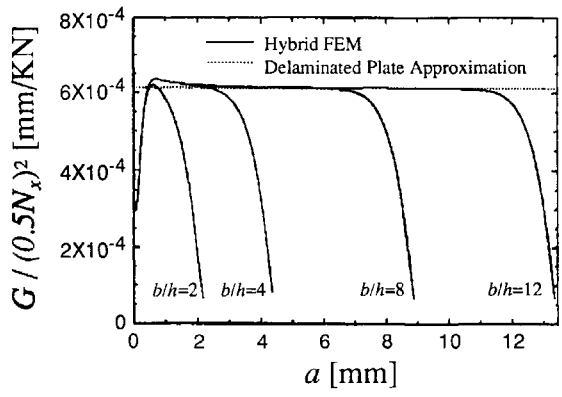

Figure 11. Potential energy release rate *vs* delamination length for graphite epoxy $[0°/90°]_S$ laminate under plane strain extension.

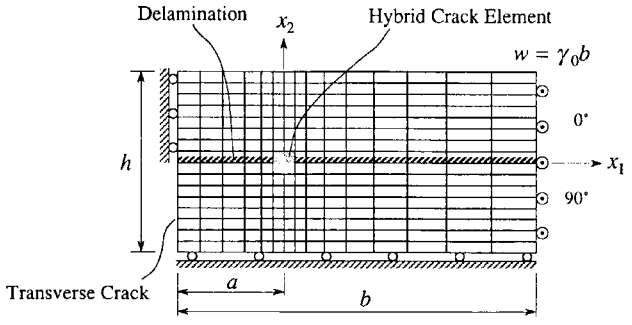

Figure 12. Graphite epoxy $[0°/90°]_S$ laminate with delamination originating from transverse crack tip under antiplane shear.

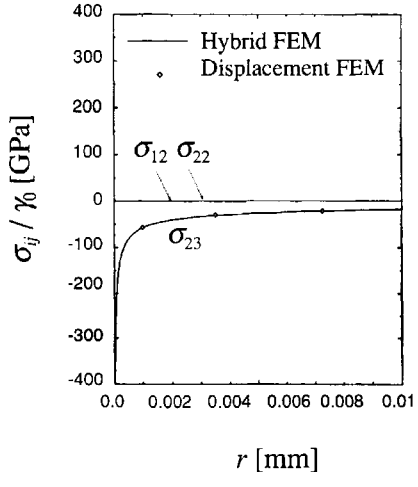

Figure 13. Stress distribution along interface of graphite epoxy $[0°/90°]_S$ laminate with delamination originating from transverse crack tip under antiplane shear.

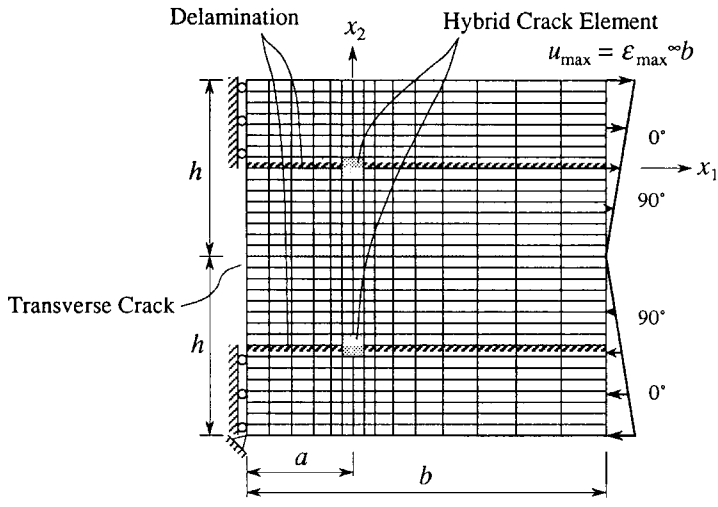

Figure 14. Graphite epoxy $[0°/90°]_S$ laminate with delamination originating from transverse crack tip under plane strain bending.

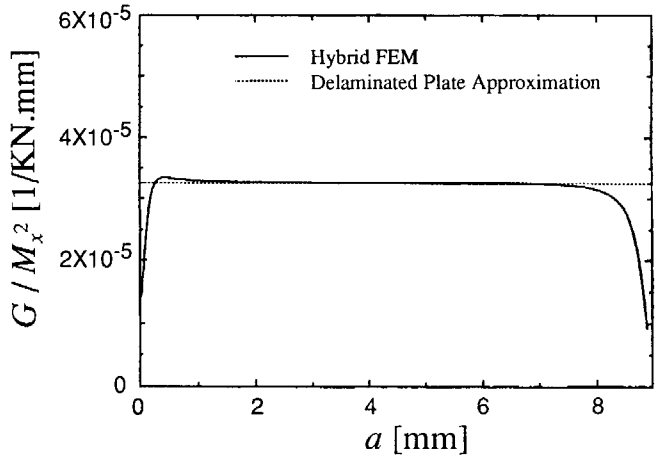

Figure 15. Potential energy release rate *vs* delamination length for graphite epoxy $[0°/90°]_S$ laminate under plane strain bending.

4.5. Laminates under plane strain bending

We analyze graphite epoxy $[0°/90°]_S$ laminate under plane strain bending by discretizing a half of the laminate as shown in Fig. 14. The potential energy release rates are shown in Fig. 15 together with the asymptotic value [7].

5. CONCLUSIONS

A hybrid crack element for analyzing an interfacial crack between unidirectional composite layers with arbitrary fiber directions has been developed based on the

asymptotic elastic solutions at the crack tip and the variational principle of a hybrid functional. Graphite epoxy laminates with delamination originating from the tips of transverse crack in cross-ply subjected to plane strain extension, antiplane shear, and plane strain bending have been analyzed by the hybrid singular element at the crack tip and the surrounding displacement-based regular elements. Numerical results for the stress distributions near the delamination tip and the potential energy release rates associated with the delamination growth have demonstrated the accuracy and efficiency of the present hybrid singular finite element method.

REFERENCES

1. K. Kondo and T. Aoki, An energy release rate approach for free-edge delamination problem in composite laminates, in: *Composite Structures 4, Proc. 4th Intnl Conf. Compos. Struct.*, I. H. Marshall (Ed.), Vol. 2, pp. 241–257, Paisley (1987).
2. K. Kondo and Y. Yasue, Transverse crack and delamination in composite laminates subjected to mechanical and hygrothermal loading, in: *Proc. 7th Japan–US Conf. Compos. Mater.*, I. Kimpara, H. Miyairi and N. Takeda (Eds), pp. 91–98, Kyoto (1995).
3. S. S. Wang and F. G. Yuan, A singular hybrid finite element analysis of boundary stresses in composite laminate, *Int. J. Solids Structures* **30**, 825–837 (1993).
4. Y. Kim and S. Im, Delamination crack originating from transverse cracking in cross-ply laminates under various loadings, *Int. J. Solids Structures* **30**, 2143–2161 (1993).
5. T. C. Ting, Explicit solution and invariance of the singularities at an interface crack in anisotropic composite, *Int. J. Solids Structures* **22**, 965–983 (1986).
6. J. Qu and J. L. Bassani, Interfacial fracture mechanics for anisotropic biomaterials, *J. Appl. Mech.* **60**, 422–431 (1993).
7. K. Kondo, Delamination of laminates subjected to mechanical and hygrothermal loadings, in: *Proc. 10th Intnl Conf. Compos. Mater.*, A. Poursartip and K. N. Street (Eds), Vol. I, pp. 213–220, Whistler (1995).
8. K. Kondo and K. Yagi, A singular hybrid finite element analysis of interlaminar crack problems, in: *Proc. 11th Intnl Conf. Compos. Mater.*, M. L. Scott (Ed.), Vol. II, pp. 290–300, Gold Coast (1997).
9. A. N. Stroh, Dislocation and cracks in anisotropic elasticity, *Philos. Mag.* **7**, 625–646 (1958).